An investigation of the electrical and optical properties of thin iron layers grown on the epitaxial Si(111)-(2 × 2)–Fe phase and on an Si(111)7 × 7 surface

D L Goroshko[1]**, N G Galkin**[1]**, D V Fomin**[2]**, A S Gouralnik**[1] **and S V Vavanova**[1]

[1] Institute of Automation and Control Processes of the Far Eastern Branch of the Russian Academy of Sciences, Vladivostok, Russia
[2] Department of Engineering and Physics, Amur State University, Blagoveshchensk, Amur Region, Russia

E-mail: goroshko@mail.dvo.ru

Abstract
Electrical and optical properties of thin iron layers grown at room temperature on the epitaxial silicide Si(111)-(2 × 2)–Fe phase and on an Si(111)7 × 7 surface were investigated using *in situ* Hall effect registration, atomic force microscopy, and optical spectroscopy. It was established that Si(111)-(2 × 2)–Fe phase has semiconducting properties with a 0.99 eV effective band gap and acts as a diffusion barrier for the deposited iron atoms, preventing intermixing with the substrate at room temperature. Peculiarities in the optical spectra of a sample with a 2 nm iron film grown on the Si(111)-(2 × 2)–Fe phase typical for both metal and semiconducting natures prove a conservation of the phase under the iron layer. The process of iron growth on the Si(111)-(2 × 2)–Fe phase is accompanied by the development of high stress in the subsurface area resulting in band dispersion changes. Apparently the tension reaches a maximum at an iron layer thickness of 1.35 nm, and a high effective hole mobility equal to 820 cm^2 V^{-1} s^{-1} was registered.

1. Introduction

Thin iron silicide phases on silicon have attracted interest in the last few years. Recent investigations revealed that epitaxial Si(111)c(4 × 8)–Fe iron silicide [1, 2] can be obtained from Si(111)-(2 × 2)–Fe in the narrow iron coverage range (1.5–1.7 ML) at temperatures of 550–600 °C. Both phases do not contain any foreign atoms and are rather stable. They have very smooth and flat Si-terminated surfaces with regularly arranged vacancies. But their electrical properties under ultrahigh vacuum conditions (*in situ*) have not yet been studied.

In situ Hall effect measurements have usually been devoted to investigation of the transport properties of two-dimensional (2D) metal layers and surface phases on silicon [3–5]. Non-siliciding materials like Pb [4], Ag, and Au [5] were mainly studied in experimental works. An understanding of conductance mechanisms in the silicon–transition metal system at Hall effect measurements is complicated because of silicide formation at the interface [6]. The first experiments on Hall measurements during Si(111)–Fe and Si(111)–Cr interface formation [3] revealed a strong influence of the substrate type on the results. It was found that the Hall voltage changes sign at small iron coverage grown on an n-type silicon substrate and resistance increases on a p-type one.

It was proposed in [1] that an epitaxial Si(111)c(4 × 8)–Fe phase could be the template for epitaxial growth at high substrate temperature of semiconducting iron silicide—a prospective material for silicon optoelectronics. We guess that at room temperature the Si(111)c(4 × 8)–Fe and Si(111)-(2 × 2)–Fe phases look very interesting as possible precursors for thin iron films grown on silicon due to the possibilities

of integrating them as the magnetic memory media into the traditional silicon technology and their possible applications in spintronics. Analogous behavior has been observed for Si(111) $(\sqrt{3} \times \sqrt{3})$–B [7] and Si(111) $(\sqrt{3} \times \sqrt{3})$–Cr [8] surface phases as precursors in the Si(111)–Fe system.

In view of possible applications, a shortage of the required information on electrophysical properties (carrier mobility, carrier concentration, resistivity) for the Si(111)-(2 × 2)–Fe/Fe system is obvious. So, *in situ* Hall measurements for the Si(111)-(2 × 2)–Fe/Fe system at different stages of the Fe deposition at room temperature can give information about transport mechanisms in this system and changes of its interface and growth mechanism. The main methodical complexity of experimental data interpretation in such a Si-metal system is a correct consideration of the substrate shunting effect and space charged layer. It is known that the conductance of an atomically clean silicon sample consists of the mentioned components [9] plus a conductance through surface states, if they are arranged in a 2D band with some density of states [10]. These mechanisms of carrier transport must be taken into account in the process of data interpretation for the Si(111)-(2 × 2)–Fe/Fe system.

In the present work carrier transport in ultrathin iron films grown on the Si(111)-(2 × 2)–Fe and Si(111)-(7 × 7) phases is studied by *in situ* Hall effect measurements during the growth process at room temperature, including the *in situ* Hall measurements on the Si(111)-(2 × 2)–Fe phase and clean Si(111) substrate at elevated temperatures.

2. Experiment

The growth experiments were performed in an ultrahigh vacuum (UHV) system with a base pressure of 1×10^{-9} Torr. The UHV chamber is equipped with an iron source (99.99%), sublimation source of silicon (boron doped, 1 Ω cm), a quartz thickness sensor, low-energy electron diffraction (LEED) analyzer, and an automated facility for *in situ* Hall measurements [11, 12]. The sample, a Si(111) bar with dimensions of $17 \times 5 \times 0.35$ mm^3, boron doped with resistivity 1 Ω cm, was mounted in a sample holder, which allowed indirect heating up to 270 °C. The silicon sample was chemically cleaned in organic solvent before loading into the UHV chamber. Then it was out-gassed at 650 °C for 8 h and cooled down to room temperature. An atomically clean surface Si(111)7 × 7 of the sample was obtained after flashes at 1250 °C. After this cleaning procedure the sample demonstrated a sharp (7 × 7) LEED pattern, indicating atomic cleanliness of the surface. In some experiments an additional epitaxial layer of 100 nm Si was grown at 750 °C. Formation of the ordered iron surface phase was performed by solid phase epitaxy at 600 °C according to [1, 2]. Iron was evaporated from the DC-heated well out-gassed tungsten spiral. The deposition rate $V_{Fe} \sim (0.15–0.20)$ nm min^{-1} was calibrated with the quartz thickness sensor before and after each experiment. We estimate the iron deposition portion reproducibility as 20%.

Iron was deposited on the atomically clean Si(111)7 × 7 surface or on the prefabricated epitaxial silicide (Si(111) 2 × 2–Fe phase) at room temperature by a discrete portion of 0.1 nm.

Electrical measurements were performed on the atomically clean surface, after the formation of Si(111) 2 × 2–Fe phase and after deposition of each iron portion. A Hall voltage (U_H) and longitudinal voltage (U_ρ) proportional to resistance were registered. Three or four repetitive adjustments were made to evaluate an inaccuracy originating from a possible shift of probes since after each iron deposition a sample re-contacted with a probe measuring head [11]. The data were averaged and a root mean square deviation was calculated. The errors did not exceed 5% for the worst case. The measurements at raised temperatures in the range 20–270 °C were made using an automated two-frequency method [12] during cooling down of the sample.

Three samples were studied: two films grown on the prefabricated Si(111)-(2 × 2)–Fe phase and one film grown on the Si(111)-(7 × 7) sample for comparison. After completion of the electrophysical measurements, the morphology of each sample was studied *ex situ* on an atomic force microscope (AFM) Solver P 47 immediately after unloading from the UHV chamber. Optical properties of the iron films were calculated from transmission and reflectance spectra which were registered *ex situ* on Hitachi U-3010 and Solar TII MSDD1000 spectrophotometers.

3. Results and discussion

3.1. Formation and morphology of Si(111)-(2 × 2)–Fe phase

It is known that exact iron coverage in the range 0.15–0.17 nm grown at room temperature followed by annealing at 550–600 °C is required for the formation of Si(111)c(4 × 8)–Fe phase [1, 2]. Because of low iron deposition portion reproducibility, the formation of the phase was carried out by deposition of an increasing iron portion (0.05–0.3 nm according to our estimation) at room temperature and by annealing at 600 °C. Each step was controlled by LEED. In the case of phase formation failure a flash was made followed by 100 nm silicon epitaxial growth for surface regeneration. After this procedure a sharp 7 × 7 LEED pattern was observed. Unfortunately, only the bright 2 × 2 LEED pattern (figure 1(b)) was registered in the temperature range and iron coverage which corresponds to the formation region of Si(111)c(4 × 8)–Fe phase. Since the structure of Si(111)c(4 × 8)–Fe surface phase is defined by the ordered mesh of iron vacancies in the FeSi$_{1+x}$ lattice (CsCl type) [13] the deposition and annealing of the iron in a vacuum of 1×10^{-9} Torr did not allow us to obtain an ordering on the surface patches larger than the coherence length of the LEED beam. A thin homogeneous silicide layer with ordering of both (2 × 2) and c(4 × 8) is terminated with Si, namely the adatom's layer with p(2 × 2) ordering is over the silicon p(1 × 1) layer [13, 14]. We guess that the Si(111)-(7 × 7) surface used as the substrate was not sufficiently perfect; prepared in the vacuum 1×10^{-9} Torr it had too many defects which did not give enough surface quality for the Si(111)-(4 × 8)–Fe phase formation because the lattice unit of this phase is rather large. The epitaxial silicide formed by the method described above will be referred to as the Si(111)-(2 × 2)–Fe or, in short, the (2 × 2)–Fe phase.
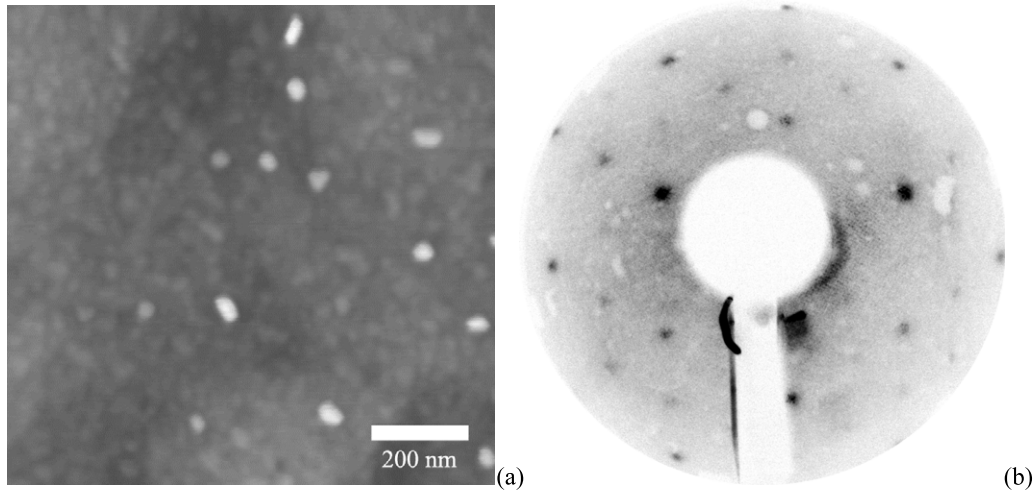
Figure 1. AFM image of the silicon sample's surface with a Si(111)-(2 × 2)–Fe phase (a) and LEED pattern registered from the surface (b). The LEED intensities have been inverted white to black.
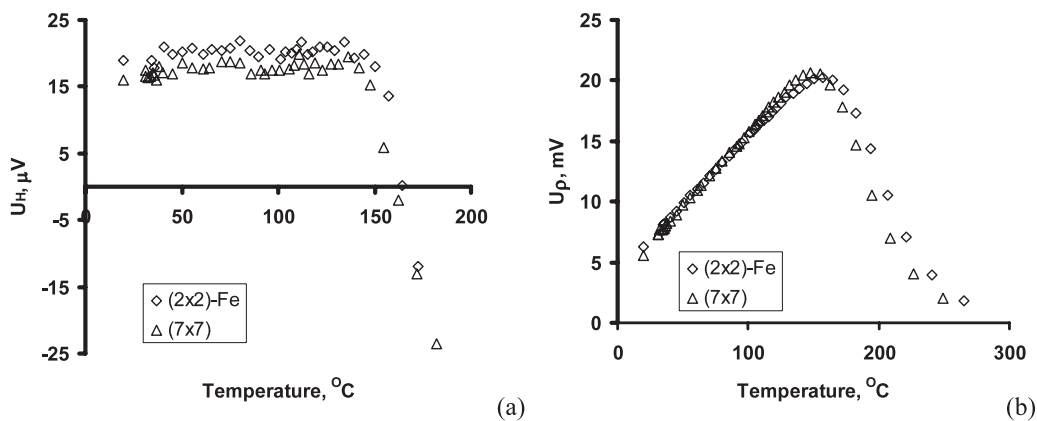

Figure 2. Hall voltage (a) and longitudinal voltage (b) versus temperature for Si(111)-(2 × 2)–Fe phase and clean silicon Si(111)-7 × 7. The RMS deviation of each data point is less than 5%.

The surface morphology of the sample with Si(111)-(2 × 2)–Fe phase with mean square root roughness of about 0.4 nm and the corresponding LEED pattern are presented in figure 1. Most of the surface is covered by a uniform layer with low roughness (0.2 nm). There are randomly ordered three-dimensional (3D) islands with sizes 20–40 nm, heights 2–3 nm, and density 1×10^9 cm^{-2} over the layer. Probably they were formed from surplus Fe and Si atoms forming a Si(111)-(2 × 2)–Fe phase [2]. Having such small sizes and density they could not provide the high intensity of the LEED spots. So, the registered LEED pattern is taken from the flat layer with root mean square (RMS) roughness 0.2 nm, consisting of 2D domains with sizes 30–50 nm and a density of 1×10^{12} cm^{-2}.

3.2. Transport properties of the Si(111)-(2 × 2)–Fe phase

In situ investigations of longitudinal and Hall voltage versus temperature (figure 2) were made on the same sample first with atomically clean Si(111)-7 × 7 and then on the ordered Si(111)-(2 × 2)–Fe phase.

It was found that at room temperature (RT) the conductance of the sample with (2 × 2)–Fe phase is lower on 2×10^{-4} Ω^{-1} (-14%) than that of the atomically clean silicon. The same was observed in the case of small iron coverage deposition on the atomically clean silicon at RT— the conductance decreased by 6% on the p-type substrate at 0.1 nm iron thickness [3]. In our experiments the alteration of conductance by an order of magnitude coincides with the result of Poisson's equation solving with regard to the space charged layer under the Si(111) surface. A recharging of localized surface states of the 7 × 7 superstructure gives rise to band bending and depletion layer formation [9]. We assign the reduction of the sample conductance after (2 × 2)–Fe growth to the formation of additional traps in the form of the defect's net of assumed Si(111)c(4 × 8)–Fe phase. This results in carrier concentration decreasing.

At temperatures above 120 °C one can notice a different character of longitudinal and Hall voltages (figure 2). A transition to intrinsic conductance in the sample with Si(111)-(2 × 2)–Fe phase occurs at a higher temperature as compared with an atomically clean silicon surface. At temperatures higher than 165 °C the resistance of sample with Si(111)-(2 × 2)–Fe phase decreases at a lower rate than that for a sample with Si(111)7 × 7 phase. At the same
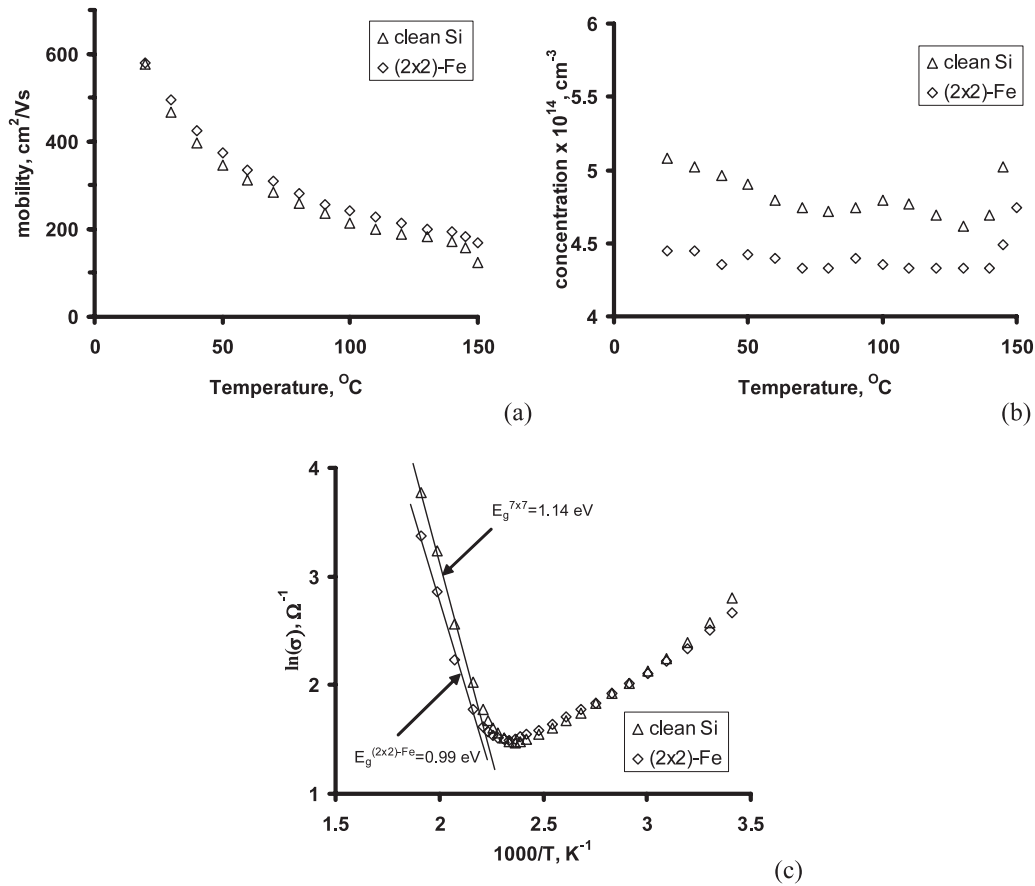
Figure 3. Results of calculation for the sample with Si(111)-(2 × 2)–Fe phase and clean Si(111)7 × 7: effective hole mobility (a) and concentration (b) as a function of the temperature. (c) Logarithm of conductance versus reciprocal temperature; a linear fit in (c) gives the band gap for the (2 × 2)–Fe phase $E_g^{(2\times 2)-Fe}$ and clean silicon $E_g^{7\times 7}$.

time one can see an increased Hall voltage (proportional to carrier mobility) for a sample with Si(111)-(2 × 2)–Fe phase.

Since the longitudinal voltage (figure 2(b)) of a sample with Si(111)-2 × 2–Fe phase is close to that of a silicon sample we cannot use a two-layer model [3]. The results of effective electrical parameter calculations for the samples with Si(111)-(2 × 2)–Fe and Si(111)7 × 7 phases assuming homogeneous bulk doping are presented in figure 3. The sample with Si(111)-(2 × 2)–Fe phase has a higher mobility of majority carriers (holes) (figure 3(a)) and a lower hole concentration (figure 3(b)) in the temperature range 20–150 °C as compared with atomically clean silicon. The temperature dependences of conductance (figure 3(c)) have a different inclination at high temperatures that corresponds to the change of effective band gap value. Decrease of the band gap value is seen for the sample with Si(111)-(2 × 2)–Fe phase. Such behavior could be possible only if a Si(111)-(2 × 2)–Fe phase has semiconducting properties with a narrow band gap. Calculations of the energy band gap of the samples with Si(111)-(2 × 2)–Fe and Si(111)7 × 7 phases from dependences of conductance versus a reverse temperature (figure 3(c)) showed that for atomically clean silicon it equals 1.14 ± 0.05 eV, but for a sample with Si(111)-(2 × 2)–Fe it decreases down to 0.99 ± 0.06 eV.

3.3. Electrical properties of thin iron coverage on Si (111)7 × 7 and Si(111)-(2 × 2)–Fe phase

Investigations of the transport properties of the iron grown on the Si(111)-(2 × 2)–Fe phase were carried out on two samples with different crystalline phase quality. The preparation procedure of the (2 × 2)–Fe phase was identical except for an annealing duration: sample A was annealed for 45 min, sample B for 20 min. At the same time, the LEED pattern of (2 × 2)–Fe phase from these two samples by spot and background intensities were indistinguishable. In order to obtain comparative data, an additional experiment was made under the same conditions (silicon substrate from which the sample was cut, vacuum, iron source, etc) on the atomically clean Si(111)7 × 7 surface—sample C.

Let us consider a Hall and longitudinal voltage evolution from the iron coverage (figure 4). Irrespective of substrate state there are common features in all the curves. For the Hall voltage there is a small reduction right after the beginning of deposition, then an increase of different intensity followed by a fall (figure 4(a)). The major changes were registered for sample A. AFM images of the surface of sample A (figure 5) revealed that the layer has low roughness (RMS 0.11 nm) and consists of flat islands with sizes of 20–30 nm. Thus, during deposition of Fe on Si(111)-(2×2)–Fe phase at RT the nucleation and growth
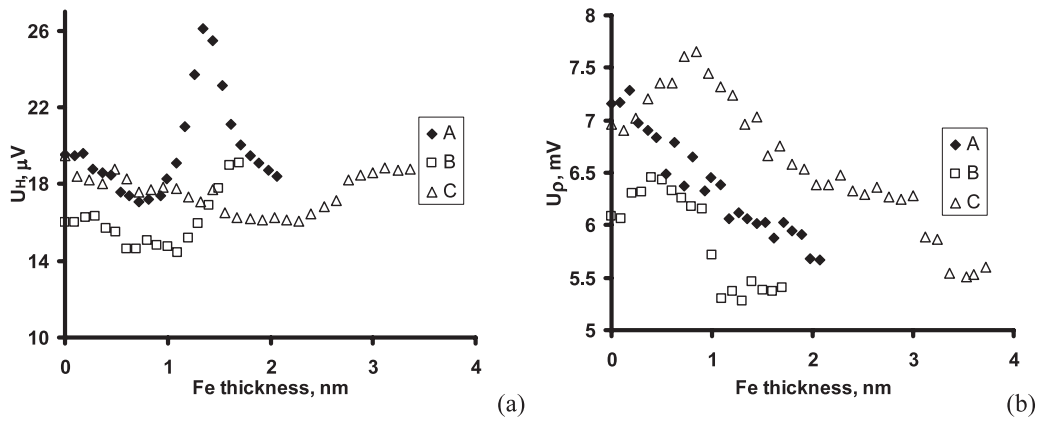
Figure 4. Hall voltage (a) and longitudinal voltage (b) versus iron thickness for the samples with prefabricated Si(111)-(2 × 2)–Fe phase annealed for 45 min (sample A) and 20 min (sample B) along with atomically clean silicon Si(111)7 × 7 (sample C). The RMS deviation of each data point is less than 5%.
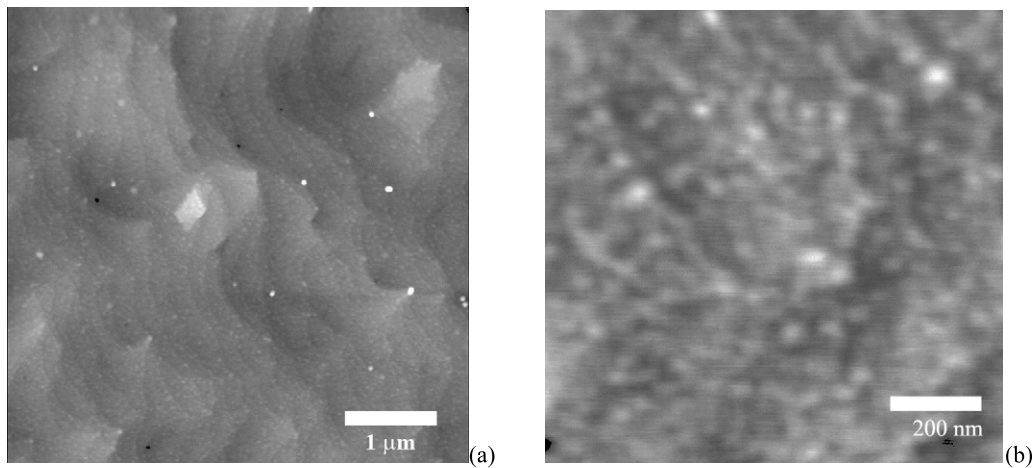

Figure 5. AFM images of the Si(111)-(2 × 2)–Fe phase with deposited iron (2 nm—sample A). The sizes are (a) 5 μm × 5 μm, (b) 1 μm × 1 μm.

of 2D islands occurs according to an island growth mode (Volmer–Weber growth mode) as previously shown in [15].

The abrupt changes of Hall voltage (figure 4(a)) for sample A indicates a strong deviation of transport properties as compared with clean silicon. A similar behavior is observed for sample B, but the height of the maximum is lower and appears at thicker coverage. While all significant changes of Hall voltage in these samples took place in the thickness range up to 2 nm, an iron layer almost twice as thick was required to register such maximum on sample C. We suppose that these changes in the Hall voltage are explained by the accumulation of stress and relaxation processes of iron silicide [15]. The strongest stress is generated in sample A with better crystalline quality. Some degradation in stoichiometry or continuity of the Si(111)-(2 × 2)–Fe phase resulted in a lighter stress in sample B. The near absence of tension as compared with samples A and B resulted in a smooth changing of Hall voltage during iron deposition on the atomically clean silicon.

As to the longitudinal voltage, which is directly proportional to resistance, it changes in two stages: a steep increase from the very beginning followed by a gradual decrease (figure 3(b)). Minimal increase is registered for sample A and maximal for sample C. An increasing of the resistance is associated with a decrease of carrier concentration on the surface during silicide formation. According to [6] this process is accompanied with an essential intermixing of deposited iron atoms and silicon resulting in the disordering of the subsurface region. This effect is strongly pronounced on sample C —a clean surface, and it is almost absent in sample A. Therefore, minimal diffusion of iron atoms occurs on the epitaxial silicide phase with the best crystalline quality (sample A). Besides, there should be a part of the silicon surface without this silicide phase in sample B. The latter could be possible due to smaller Fe coverage actually being deposited at the same deposition time (for example, smaller Fe deposition rate) on the Si(111)7 × 7 surface during the formation of the Si(111)-(2 × 2)–Fe phase.

Figure 6 shows the result of the electrical parameter calculations for sample A under the assumption of homogeneous bulk doping. In this approach we do not use complicated models taking into account the presence of multilayer structure with various types of conductivity and resistance along with possi-
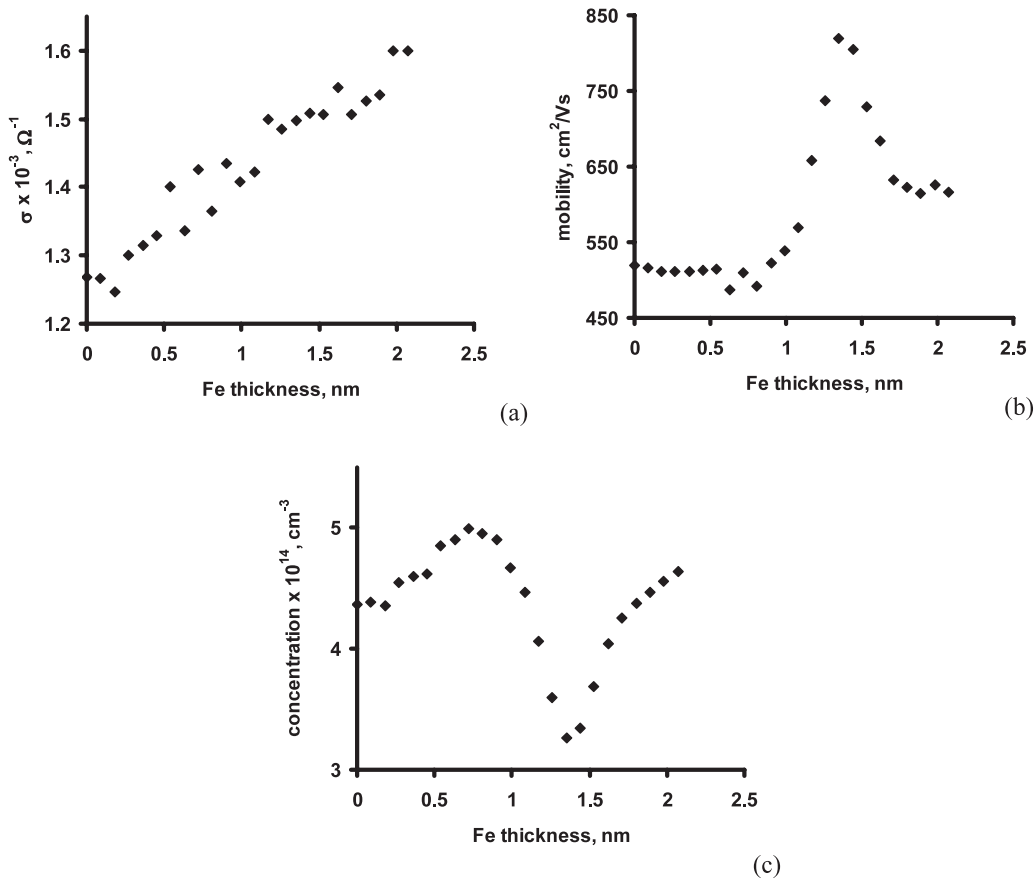
Figure 6. Results of calculation for sample A: conductance (a), effective hole mobility (b), and concentration (c) versus iron coverage.

ble p–n junction between them such as, for instance, in [16], because there is the potential of artificial figures depending on the model features. Here we calculate conductance, mobility, and concentration of majority carriers using well known, text-book Hall effect theory. These values are some kind of ef-fective characteristic of the system consisting of at least two parts—the wafer and the film. Effective values are the most reasonable interpretation of electrical properties measured us-ing macroprobes, because when the distance between probes is much more than the thickness of the sample it is hard to esti-mate the exact current distribution in the depth.

Conductance decrease of sample A at the beginning of iron deposition (0–0.2 nm) is attributed to silicide formation. The reaction takes place during the interaction of iron atoms and silicon adatoms forming a p(2×2) structure. The silicide islands start to coalescence at an iron coverage of 0.3 nm [15], which corresponds to the beginning of conductance increasing (figure 6(a)). Iron diffusion is blocked at this stage (0–0.8 nm), and the growth of iron islands with strained structure goes on further. Hole mobility slightly decreases (figure 6(b)) while its concentration increases (figure 6(c)). Therefore, silicide formation at the beginning of iron growth on the silicon at RT resulted in disordering of the subsurface region, increasing of the carrier scattering, and decreasing of conductance. This effect is the strongest on sample C (atomically clean silicon) where the decrease of conductance is observed up to 0.8 nm,

and it reaches 9%. Si(111)-(2×2)–Fe phase formation strongly reduces the intermixing. In this case iron atoms react with the silicon remaining on the surface and create 3D islands. The higher the (2×2)–Fe crystalline quality is, the less free silicon surface is left for the silicide reaction.

With further Fe deposition on Si(111)-(2×2)–Fe phase pseudomorphous growth of the iron film occurs. This film is probably highly strained, because the lattice constant of bulk iron differs from that of any iron silicide [17]. We conclude that the stress in the iron film is the reason for the drastic increase of mobility in sample A. At an iron thickness of 1.35 nm the effective mobility reaches 820 cm^2 V^{-1} s^{-1} (figure 6(b)), while the mobility at the initial state (after Si(111)-(2×2)–Fe phase formation) is 520 cm^2 V^{-1} s^{-1}. So, there is a greater than 1.5 times increase of this value in sample A. Changing of effective hole concentration (figure 6(c)) from Fe coverage corresponds to a bulk model. A decrease of hole concentration correlates with an increase of hole mobility. Note that our estimation is related to the whole sample, including a thick wafer with low carrier mobility. Keeping in mind that all changes are attributed to the very thin deposited layer, the real increase of mobility is expected to be at least one order higher. This assumption could be checked using a sophisticated measuring procedure with micro- or nanoprobe apparatus only [18].

A propagation of the stress induced by the iron film leads to the distortion of the silicon lattice in the subsurface region. A
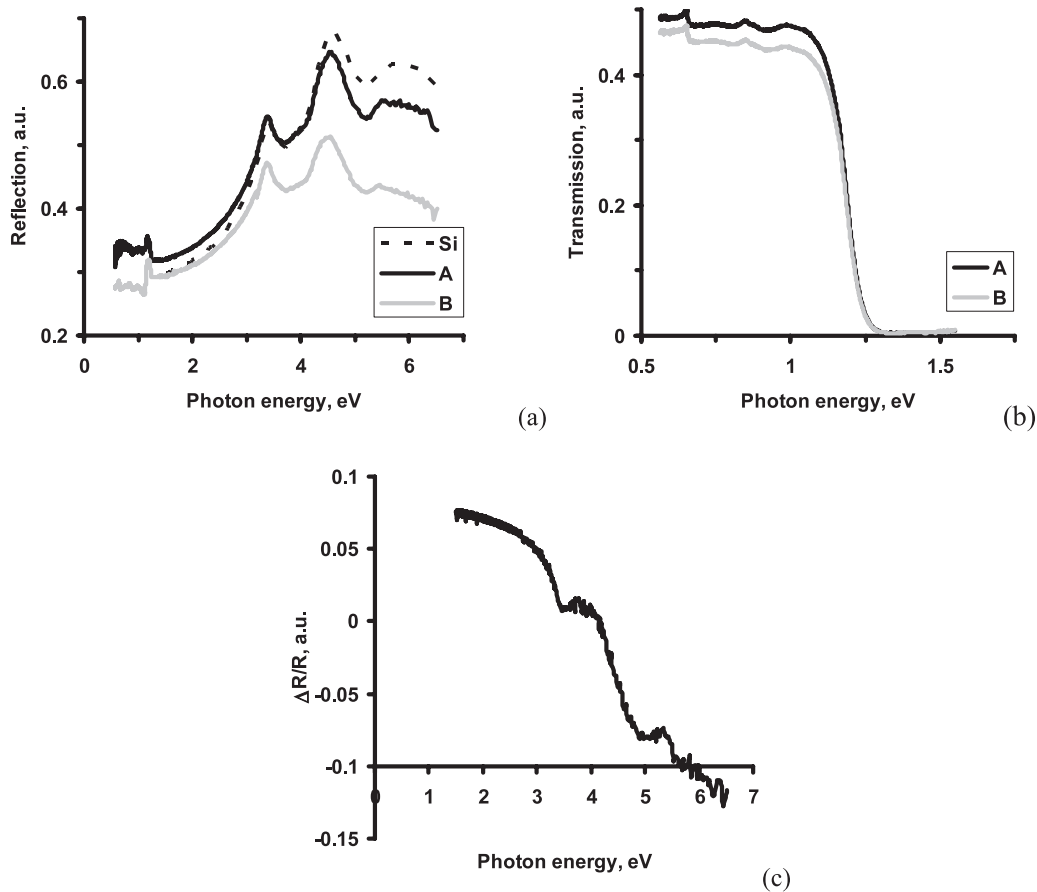
Figure 7. Reflection (a) and transmission (b) spectra of samples with different crystalline quality of Si(111)-(2 × 2)–Fe ordered phase; the reference spectrum of clean silicon denoted as Si is also shown. Differential reflectance spectrum of sample A and clean silicon (c).

strong tension of the silicon sample was reported earlier in [19] where the bending of a wafer was directly registered during iron deposition. Changes in the silicon lattice periodicity resulted in the dispersion of band structure and the appearance of valleys with light carriers. Carriers with reduced effective mass are responsible for the increase of effective mobility detected in our experiments.

A lower peak of the Hall voltage at an iron coverage of 1.7 nm (figure 4(a)) is also registered during deposition of iron on sample B, for which the Si(111)-(2 × 2)–Fe phase does not occupy all the substrate surface. Interaction of iron atoms with the bare silicon does not allow the production of a uniform iron film. The strained structure appears only on the 2D domains of the Si(111)-(2 × 2)–Fe phase. As a result, the maximum of the Hall voltage shifts to the thicker coverage. A weak maximum of the Hall voltage in the case of iron deposition on the atomically clean Si surface is observed at 3.3 nm, and its value reaches that of the initial state (figure 4(a)). The stress in such films is not very high because of a reactive interface which favors the intermixing of Fe and Si. The absence of ordered silicide at the beginning of deposition results in the formation of a more or less continuous iron film at higher thicknesses.

Stress relaxation in the iron grown on silicon with prefabricated ultrathin iron silicide begins from $d_{Fe} = 2.3$ nm, as shown in [20] by x-ray diffraction. Along with the relaxation

an epitaxial iron growth starts with lattice constants close to the bulk metal. Actually this bound could be slightly lower, because the authors in [20] used wide steps of deposited iron portions. For instance, in [15] peaks specific for bulk iron were detected in x-ray photoelectron diffraction spectra from the 1.8 nm of Fe. In our case the moment of relaxation is defined by the reactivity of the Si–Fe interface. When the film reaches some critical thickness, it relaxes. For sample A it equals 1.35 nm. It should be noted that some residual stress remains: an enlarged mobility exists after a steep fall at 1.7 nm.

3.4. Optical properties of thin iron layers on Si(111)7 × 7 and Si(111)-(2 × 2)–Fe

Transmission and reflection optical spectra were registered for the samples with iron layers on the Si(111)-(2 × 2)–Fe phase after unloading from the growth chamber (figures 7(a) and (b)). The reflection spectrum of monocrystalline silicon for the nontransparent region is also presented. It is clear that sample B with low crystalline quality has a smaller reflection coefficient in the photon energy higher than 1.5 eV as compared with silicon because of an essentially developed surface relief. Decreasing of transmission (figure 7(b)) also testifies to an enlarged dissipation on the surface. Sample A with the iron layer grown on the Si(111)-(2 × 2)–Fe phase

with good crystalline quality has, however, a higher reflectivity than silicon for the range up to 3 eV. This is confirmed by the differential reflectance spectrum (DRS) presented in figure 7(c).

A smooth decrease of the differential reflection coefficient ($\Delta R/R$) with photon energy testifies to the metal character of absorption [21], but the broad maximum at 2.7–2.8 eV and small peak at 3.8 eV correspond to the contribution of some semiconductor phase too. On the one hand, the deposition of Fe on the Si(111)-(2×2)–Fe phase at room temperature results in the conservation of the semiconductor contribution of Si(111)-(2×2)–Fe phase, which was revealed from *in situ* Hall temperature measurements (figure 3(c)). On the other hand, a metallic contribution from stressed 2D iron islands atop Si(111)-(2×2)–Fe phase also exists. So, we can speculate about the conservation of Si(111)-(2×2)–Fe phase due to the stress and absence of atomic intermixing in this system. Additional *in situ* DRS experiments are required for optical constants and energy gap calculations in the Si(111)-(2×2)–Fe phase and thin Fe covering layers.

4. Conclusions

In summary, we studied the electrophysical properties of thin iron film grown on the ordered silicide phase Si(111)-(2×2)–Fe and on the clean silicon Si(111)7 × 7 at room temperature. The Si(111)-(2×2)–Fe silicide phase proved to be a semiconducting one with a narrower band gap (0.99 ± 0.06 eV) than clean silicon (1.14 ± 0.05 eV). It was shown that the Si(111)-(2×2)–Fe phase significantly reduces intermixing of deposited iron atoms and the substrate. It leads to the formation of a pseudomorphous layer and the development of high stress in the subsurface region, resulting in a change in the band dispersion. This effect depends on the quality of the prefabricated ultrathin silicide. In the case of continuous epitaxial Si(111)-(2×2)–Fe phase formation the phenomenon is the most pronounced. We assume that the appearance of valleys in the energy band with light holes in silicon is a reason for the effective mobility increasing. At an iron thickness of 1.35 nm it reaches 820 cm^2 V^{-1} s^{-1}, which is 1.5 times higher than for the initial state. Transmission and reflection spectra of the grown films also testify to conservation of the Si(111)-(2×2)–Fe phase under the iron layer. There are features in the optical spectra reflecting the presence of semiconducting (2×2)–Fe phase along with metal properties of the iron layer upon it.

References

[1] Hajjar S, Garreau G, Pelletier S, Bolmont D and Pirri C 2003 *Phys. Rev.* B **68** 033302
[2] Kataoka K, Hattori K, Miyatake Y and Daimon H 2006 *Phys. Rev.* B **74** 155406
[3] Galkin N G, Goroshko D L, Konchenko A V, Ivanov V A, Zakharova E and Krivoshchapov S Ts 2000 *Surf. Rev. Lett.* **7** 257
[4] Vilfan I, Henzler M, Pfennigstorf O and Pfnür H 2002 *Phys. Rev.* B **66** 241306
[5] Hirahara T, Matsuda I, Liu C, Hobara R, Yoshimoto S and Hasegawa S 2006 *Phys. Rev.* B **73** 235332
[6] Alvarez J, Vázquez A L, Hinarejos J J, Figuera J, Michel E G, Ocal O and Miranda R 1993 *Phys. Rev.* B **47** 16048
[7] Ivanchenko M V, Borisenko E A, Kotlyar V G, Utas O A, Zotov A V, Saranin A A, Ustinov V V, Solin N I, Romashev L N and Lifshits V G 2006 *Surf. Sci.* **600** 2623
[8] Galkin N G, Konchenko A V, Goroshko D L, Maslov A M, Vavanova S V and Kosikov S I 2000 *Appl. Surf. Sci.* **166** 113
[9] Hasegawa S, Tong X, Takeda S, Sato N and Nagao T 1999 *Prog. Surf. Sci.* **60** 89
[10] Jiang C-S, Hasegawa S and Ino S 1996 *Phys. Rev.* B **54** 10389
[11] Galkin N G and Goroshko D L 2001 *Phys. Low-Dimens. Struct.* **9/10** 67
[12] Galkin N G, Ivanov V A, Konchenko A V and Goroshko D L 1999 *Instrum. Exp. Tech.* **42** 284
[13] Garreau G, Hajjar S, Gewinner G and Pirri C 2005 *Phys. Rev.* B **71** 193308
[14] Krause M, Blobner F, Hammer L and Heinz K 2003 *Phys. Rev.* B **68** 125306
[15] Garreau G, Hajjar S, Bubendorff J L, Pirri C, Berling D, Mehdaoui A, Stephan R, Wetzel P, Zabrocki S, Gewinner G, Boukari S and Beaurepaire E 2005 *Phys. Rev.* B **71** 094430
[16] Muret P, Ali I and Brunel M 1998 *Semicond. Sci. Technol.* **13** 1170
[17] Eggert B and Panzner G 1984 *Phys. Rev.* B **29** 2091
[18] Shiraki I, Tanabe F, Hobara R, Nagao T and Hasegawa S 2001 *Surf. Sci.* **493** 633
[19] Sander D, Enders A and Kirschner J 1995 *J. Appl. Phys. Lett.* **67** 1833
[20] Stephan R, Zabrocki S, Wetzel P, Berling D, Mehdaoui A, Bubendorff J-L, Garreau G, Pirri C, Gewinner G, Boudet N and Berar J F 2006 *Surf. Sci.* **600** 3003
[21] McIntyre J D E and Aspnes D E 1971 *Surf. Sci.* **24** 417